CRACK CLOSURE AND INITIATION STRESSES OF COAL SUBJECTED TO THERMO-GAS-MECHANICAL COUPLING

by

Yanan GAO [a,b*], ***Weicheng YAN*** [a,b], ***and Xiaojun YANG*** [a,b]

[a] State Key Laboratory for Geomechanics and Deep Underground Engineering, China University of Mining and Technology, Xuzhou, China
[b] School of Mechanics and Civil Engineering, China University of Mining and Technology, Xuzhou, China

Original scientific paper
https://doi.org/10.2298/TSCI17S1301G

In this paper, the orthogonal experiment method is employed to design physical tests of coal under different temperatures, confining pressures, and gas pressures. The crack closure stress and crack initiation stress are calculated using four known methods, i. e. axial strain method, axial stiffness method, crack volume method, and strain response method. The obtained results are compared, and the advantages and drawbacks for the used methods are also discussed. The influences of the three factors on the crack closure and crack initiation stresses are analyzed.

Key words: *temperature, mechanical test, crack closure stress, crack initiation stress*

Introduction

Due to the complex deformation patterns in the deep coal and rock, the coal-and-gas-outburst and roof caving could cause serious damage [1]. The deformation and failure of coal and rock could be the result of crack initiation and propagation [2]. Ground temperature, ground stress, and gas pressure affect the mechanical properties of coal and rock, which influence the formation and development of coal and rock cracks [3]. Understanding the influence of temperature, ground stress, and gas pressure on crack evolution in coal and rock can help reveal the mechanism of deformation and failure of coal and rock.

The coal and rock failure process can be divided into four stress states based on the processes of crack closure, initiation, propagation, and coalescence: crack closure stress, crack initiation stress, damage stress, and peak stress stages [4]. Recent studies in rock mechanics examined stress thresholds in coal and rock failure. The crack volumetric (CV), strain response (SR), axial strain (AStr), and axial stiffness (Asti) methods were considered in [5]. The relationship between the crack closure stress and sampling depth was studied in [6]. Comparison between the acoustic emission (AE) method and the lateral SR method using triaxial axis tests was made in [7].

Temperature, confining pressure, gas, and other factors may influence the mechanical properties of coal. When the confining pressure rises, the strength, Poisson’s ratio, and elastic modulus of coal gradually increase [8, 9]. The structural thermal stress causes damage to coal

* Corresponding author, e-mail: yngao@cumt.edu.cn

specimens [10]. Coal contains two types of gases: free gas and adsorbed gas [11]. Each gas has a different effect on the coal and rock deformation and intensity [3, 9].

To develop further our understanding of the changes and characteristics of crack closure stress and crack initiation stress of coal, we will use the orthogonal experiment (OE) method to design the coal and rock tests at different temperatures, confining pressures, and gas pressures and to plan to obtain the crack closure stress and crack initiation stress. The influence of the temperature and the confining and gas pressures on the crack closure stress and crack initiation stress of coal and rock are analyzed in detail.

Experiment design

The orthogonal table is the basic tool of the orthogonal test, which is based on the combination theory [11]. In order to make use of OE method in this paper, the orthogonal table designed for this study is shown as tab. 1.

Table 1. Design of orthogonal table

Group No.	T [°C]	G [MPa]	C [MPa]
M20-0-0	20	0	0
M20-1-4	20	1	4
M20-3-8	20	3	8
M40-0-4	40	0	4
M40-1-8	40	1	8
M40-3-0	40	3	0
M80-0-8	80	0	8
M80-1-0	80	1	0
M80-3-4	80	3	4

Three specimens are tested in each group. The group number denotes the test conditions (temperature and pressure) of the group, for example, M-20-3-8 indicates that this group of specimens will be tested at a temperature of 20 °C, gas pressure of 3 MPa, and confining pressure of 8 MPa. Two approaches used in orthogonal test results, for example, intuitive analysis and variance analysis, are considered. The mathematics model for the orthogonal test can be written:

$$\left.\begin{aligned} k_1 &= \alpha + T_1 + G_1 + C_1 + \eta_1 \\ k_2 &= \alpha + T_1 + G_2 + C_2 + \eta_2 \\ k_3 &= \alpha + T_1 + G_3 + C_3 + \eta_3 \\ &\vdots \\ k_n &= \alpha + T_i + G_j + C_k + \eta_n \end{aligned}\right\} \tag{1}$$

where η_i (i = 1, 2, 3... n and n is the number of observations) are independent random variables, α – the constant, k – the sum of the variables, and T_i, G_i, and C_i (i = 1, 2, 3) represent the effects of the temperature, gas pressure, and confining pressure, respectively. The S_{total} denoted as the sum of the square of all the deviations, is comprised as four terms: S_E, S_T, S_G, and S_C, where S_E is the variance produced by errors, and S_T, S_G, and S_C are the variances caused by the temperature, gas pressure, and confining pressure, respectively.

$$\left.\begin{aligned} & S_{\text{total}} = \sum_{i1=1}^{n}(k_{i1}-\bar{k})^2 = \sum_{i1=1}^{n}(k_{i1})^2 - \delta, \quad S_T = \frac{\sum_{i2=1}^{h}(M_{Ti2})^2}{Rr} - \delta, \quad S_G = \frac{\sum_{i2=1}^{h}(M_{Gi2})^2}{Rr} - \delta \\ & S_C = \frac{\sum_{i2=1}^{h}(M_{Ci2})^2}{Rr} - \delta, \quad S_E = S_{\text{total}} - S_T - S_G - S_C, \quad \delta = \frac{(\sum_{ii=1}^{n} k_{ii})^2}{n}, \quad \bar{k} = \frac{\sum_{ii=1}^{n} k_{ii}}{n} \end{aligned}\right\} \tag{2}$$

where h is the number of levels of each factor, and R and r – the number of factors and levels, respectively, M_{Ti2} – the sum of the observed quantity at level $i2$ of temperature T, while M_{Ci2} and M_{Hi2} denote similar sums for the confining gas pressure C and gas pressure H.

The coal samples were obtained from the Shoushan mine in Xuchang, Henan Province, China, displayed in fig. 1. The depth of the working face is about 600 m, the gas pressure is about 2 MPa. The X-ray diffraction analysis, illustrated in fig. 2, shows that the main components of the coal samples are calcite, kaolinite, and quartz.

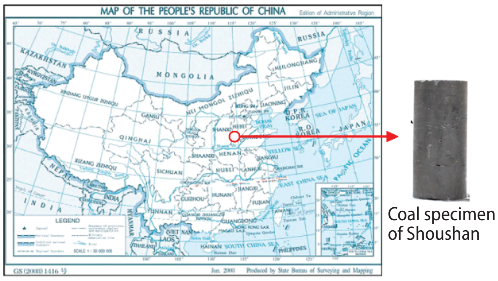

Figure 1. Location of the sampling site

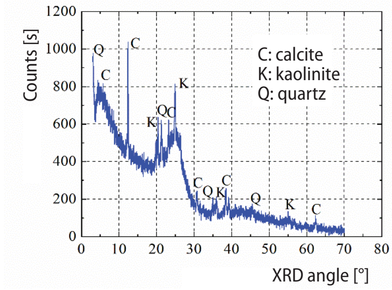

Figure 2. Results of X-ray diffraction test

The specimens were prepared in accordance with the ISRM standards [12]. After the dimensions of the prepared specimens were measured, the specimens were placed in a 100 °C oven for 24 hours. The test was performed using a TAW-2000 servo-controlled rock triaxial testing apparatus and a pulse gas meter shown in fig. 3.

Determining σ_{cc} and σ_{ci} using various methods

The deformation and failure of coal and rock involves the process of crack initiation and propagation. When coal is subjected to stress, the inner pores and fractures are initially closed by external forces. As the axial stress increases, the inner cavities and fracture boundaries lead to the formation of areas of stress concentration. When the stress concentration exceeds the coal strength limit, local cracks develop. The stress concentration is subsequently transferred to a new crack tip until the crack propagates through the specimen. The stress–strain curve of a specimen under compression before specimen failure can be divided into four stages [4]: compression of closed cracks stage, elastic stage, crack initiation to stable expansion stage, and crack unsteady expansion stage shown in fig. 3.

The AStr method

The stress-strain curve of a coal specimen tested under compression, shown in fig. 4, is non-linear at the compaction stage, and its slope increases with AStr. The tangent line of the linear phase intersects the stress-strain curve at two points, which represent the crack closure stress and crack initiation stress. The AStr method is applicable to specimens, which show non-linear behavior in the compression stage and the stable crack propa-

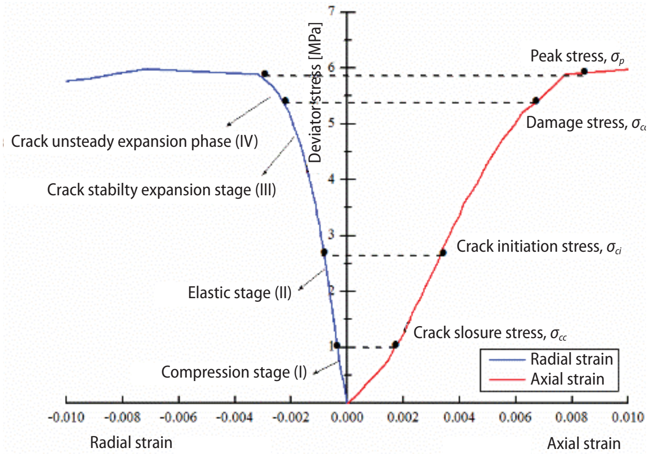

Figure 3. Stress-strain curve of a specimen under compression showing the crack development leading to failure

gation stage. However, it is difficult to determine two points representing crack closure and initiation stresses.

The ASti method

To investigate the stress thresholds of crack initiation and propagation in brittle rocks, Eberhardt *et al.* [13] proposed ASti method to obtain the crack initiation stress. The stress-strain curve indicates that with increasing stress, the axial-strain curve is initially non-linear (crack closure) then becomes linear (elastic deformation), and finally becomes non-linear again (crack initiation). As shown in fig. 5, when ASti initially increased with increasing stress, it fluctuates around a certain value, and finally gradually decreases. On ASti curve, the crack closure stress and crack initiation stress can be determined by the points marking the beginning and end of the fluctuation zone which appears around the peak of the curve. However, because of the large fluctuations of the curve, it is difficult to determine these points. Thus, the ASti method is inaccurate.

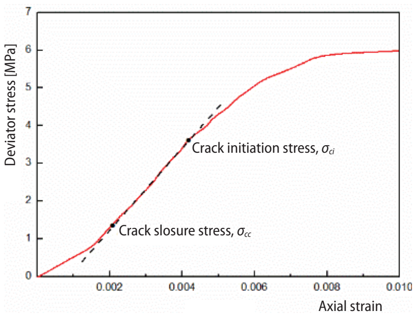

Figure 4. Stress-strain curve by AStr method

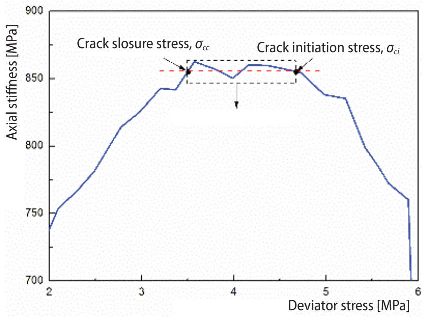

Figure 5. Stiffness-stress curve by ASti method

The CV method

Martin *et al.* [14] employed the CV method to determine the crack initiation stress and crack closure stress. The CV strain can be obtained from the total volumetric strain and the elastic volumetric strain. The CV strain-stress curve, illustrated in fig. 6, has a horizontal section which remains constant with increasing stress. The stresses corresponding to the beginning and end of the horizontal section indicate the crack closure stress and crack initiation stress, respectively.

The total volumetric strain developed during rock compression, denoted by ε_v, can be expressed as:

$$\varepsilon_v = \varepsilon_v^c + \varepsilon_v^e \tag{3}$$

where the elastic volumetric strain ε_v^e is:

$$\varepsilon_v^e = \frac{(1-2\mu)(\sigma_1 + 2\sigma_3)}{E} \tag{4}$$

and CV strain ε_v^c is given by:

$$\varepsilon_v^c = \varepsilon_v - \frac{(1-2\mu)(\sigma_1 + 2\sigma_3)}{E} \tag{5}$$

with the axial stress, σ_1, the confining pressure, σ_3, the elastic modulus, E, and the Poissons ratio, μ.

The SR method

Nicksiar *et al.* [15] proposed the use of the lateral SR to derive the crack initiation stress, and validated the SR method by comparing with other methods, such as the CV, ASti, and AE methods. Based on this method, Peng *et al.* [6] presented the AStr method to determine the crack closure stress, fig. 7.

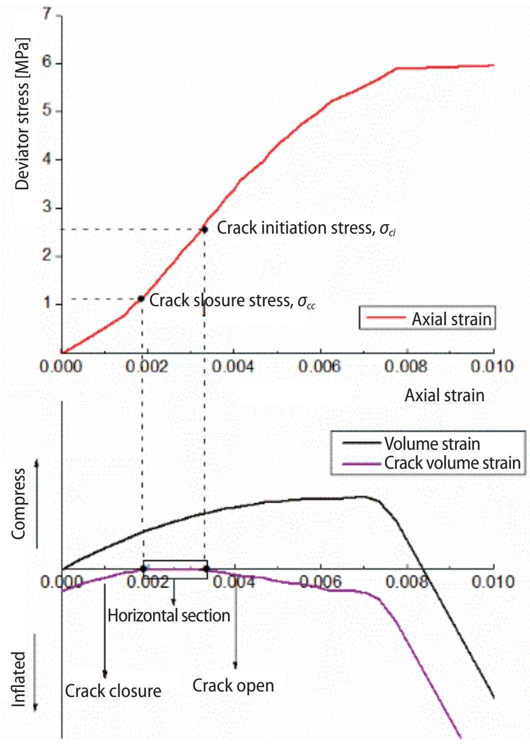

Figure 6. Stress-strain curve produced by CV method

Result and discussion

The crack closure and crack initiation stresses measured in the coal samples in the uniaxial tests using the four methods are shown in tab. 2. The coal specimens contain a large number of primary fractures, since the compaction stage is more obvious in the uniaxial tests, where the inflection points can be determined accurately. When the confining pressure is applied, the primary fractures in the coal samples are compacted, and the non-linear compacted stage is not obvious. Therefore, it is difficult to identify the inflection point between the non-linear phase and the linear phase, leading to inaccuracies in the results. The σ_{ci} can be determined by identifying the generation of new cracks and the expansion of the primary cracks. When the stress-strain curve exhibits more non-linear tendencies under uniaxial compression, it is more accurate to determine σ_{ci}.

Table 2. The σ_{cc} and σ_{ci} of the coal specimens calculated by the four methods

Group No.	①		②		③		④		⑤	
	σ_{cc}	σ_{ci}	σ_{cc}	σ_{ci}	σ_{cc}	σ_{ci}	σ_{cc}	σ_{ci}	σ_{cc}	σ_{ci}
20-0-01	1.88	3.70	3.50▲	5.70▲	1.04▽	2.40▽	1.46	3.20	1.97	3.75
20-1-43	3.37	7.74	2.19▽	4.43▽	3.36	8.20▲	3.60▲	7.34	3.13	6.93
20-3-81	5.50	17.60▲	4.53▽	10.60▽	5.58▲	13.78	5.43	14.12	5.26	14.03
40-0-43	2.42	4.60▲	2.50	4.23▽	2.96▲	4.24	2.40▽	4.50	2.57	4.39
40-1-82	3.80	9.20	4.07▽	8.59	4.40▲	10.30	3.77▽	11.00▲	4.01	9.77
40-3-04	1.78	3.57	1.25	4.53▽	1.25▽	3.80	2.30▲	4.39▲	1.65	4.07
80-0-82	2.09	4.46▽	2.60	6.80	1.56▽	4.46▽	3.42▲	12.34▲	2.42	7.02
80-1-02	2.00	3.50	1.70▽	4.30▽	2.65▲	3.27▲	2.15	4.59	2.13	3.92
80-3-43	2.23	8.57	3.80▲	9.90	2.19▽	6.47▽	2.49	9.92▲	2.68	8.72

① AStr method, ② ASti method, ③ Crack volume strain method, ④ SR method, ⑤ Mean values
▲, ▽ Maximum and Minimum value of σ_{cc} or σ_{ci}.

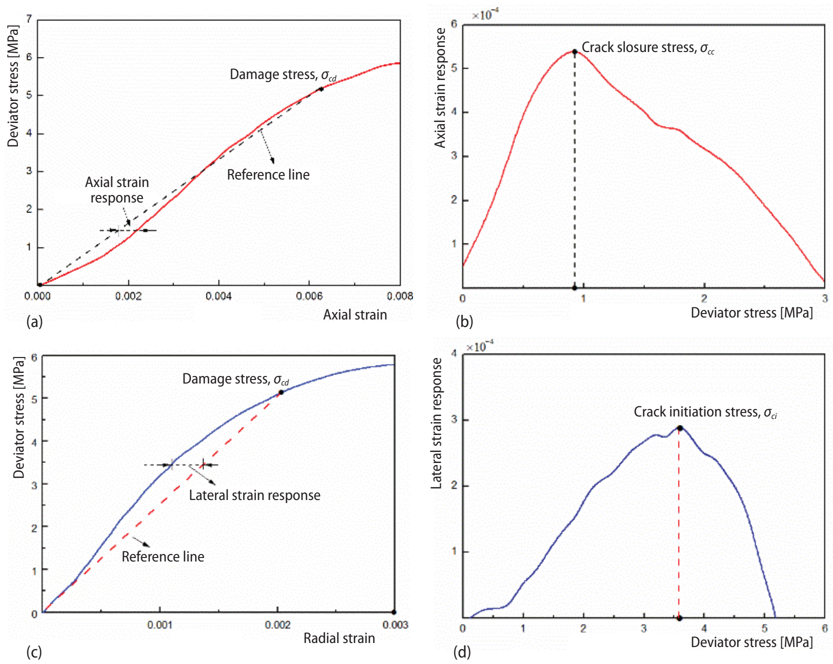

Figure 7. Stress-strain curves produced by the AStr method

The results of ASti method are influenced by temperature. As the temperature rises, the number of inner micro-cracks increases due to the thermal stress, and the distribution of cracks relatively uniforms with respect to the original fissures. Non-uniform distribution of cracks may cause fluctuations in stiffness. The CV method and SR method are also affected by temperature. The accuracy of the results of CV method depends on the accuracy of the values μ and E for each specimen. An increase in the number of micro-cracks in the coal specimen caused by a rise in temperature may affect the values μ and E [14]. The SR method has no clear physical meaning. When the temperature rises, the SR method yields poor for σ_{cc} and σ_{ci}.

To examine the effects of the pressures and temperature, we calculated the deviation of the factors, C, G, and T from the average for each method. The σ_{cc} is most affected by the confining pressure, with a significance level above 95%. The significance level of the temperature is 83.8%, and that of the gas is 62.1%, tab. 3. The σ_{ci} is most affected by the confining pressure and gas, listed in tab. 3, with a significance level of 95% and 90%, respectively, while the effect of temperature on the σ_{ci} has very low significance.

Table 3. Statistical analysis of σ_{cc} and σ_{ci} for each factor

Factor	Squared sum of deviation σ_{cc}, σ_{ci}	df	Significance level σ_{cc}, σ_{ci}
C	9.866, 88.813	2	0.002, 0.001
G	0.919, 21.715	2	0.379, 0.075
T	1.868, 3.736	2	0.162, 0.581
Error	4.762, 36.056	11	
Total	183.460, 1048.212	18	

The variance analysis for σ_{cc} and σ_{ci} indicates that the confining pressure, temperature, and gas are important factors affecting on coal deformation and strength. The confining pressure limits the lateral deformation which is caused by the expansion of the inner cracks. A rise in temperature may cause the internal damage of the coal specimens, and the axial stress may decrease once the internal cracks close. The gas affects the coal specimens mainly during the elastic phase. The free gas in the fractures reduces the effective strength of the coal specimens.

From tab. 3, we can obtain the equations of the forms:

$$\sigma_{\mathrm{cc}} = 2.536 + 0.22C - 0.013T + 0.168G \tag{6}$$

and

$$\sigma_{\mathrm{ci}} = 4.101 + 0.667C - 0.18T + 0.855G \tag{7}$$

The linear models are used to describe the variation of σ_{cc} and σ_{ci} under the combined action of the three factors, not taking into account the coupling effect between the factors. The σ_{cc} and σ_{ci} are independent variables. The C and G are positively correlated with σ_{cc} and σ_{ci}, while T is negatively correlated with the stresses. The C and G have the strongest influence on σ_{cc} and σ_{ci} . The significant level of C on σ_{cc} and σ_{ci} is above 95%, and the significance of G on σ_{ci} and T on σ_{ci} are more than 95% and 90%, respectively.

Conclusion

In this work, by determining the stress threshold during the rock failure process, we obtained the crack closure stress and crack initiation stress of coal and rock under varying temperature, gas pressure, and confining pressure. The AStr method is effective for uniaxial tests. The ASti method is suitable for high temperature tests. The crack volume method and SR method are suitable for room temperature tests. It is shown that the effects of the confining pressure on σ_{cc} and σ_{ci} are above the 95% significance level while the effects of gas pressure on σ_{ci} and temperature on σ_{cc} are at significance level of more than 95% and 90%, and by using the linear model for describing the behavior of σ_{cc} and σ_{ci} of the coal specimens under confining pressure, temperature, and gas pressure, the confining pressure and the gas pressure were positively correlated with σ_{cc} and σ_{ci} while the temperature was negatively correlated.

Acknowledgment

The work in this paper is financially supported by the National Natural Science Foundation of China (Grant No. 51404250), the Fundamental Research Funds for the Central Universities (Grant No. 2013QNB19), the China Postdoctoral Science Foundation (2014M550316, 2016T90526), the State Key Research and Development Program of China (2016YFC0600705). The authors gratefully acknowledge the financial support of the aforementioned agencies.

Nomenclature

C – confining gas pressure, [Nm^{-2}]
G – gas pressure, [Nm^{-2}]
M_{Ti2} – sum of observed quantity [Nm^{-2}]
R – number of factors in testing, [–]
r – number of levels in testing, [–]
S_C – variances due to confining pressure, [–]
S_G – variances due to gas pressure, [–]
S_T – variances due to temperature, [–]
T – temperature, [K]

Greek symbols

η_i – independent random variables, [–]
ε_v^c – the crack volumetric strain, [–]
ε_v^e – elastic volumetric strain, [–]

References

[1] Xie, H., *et al.*, Research and Consideration on Coal Deep Mining and Ultimate Mining Depth, *Journal of Coal Science*, *36* (2012), 4, pp. 535-542
[2] Liu, D., *et al.*, Study on Dynamic Monitoring of Rock Crack Propagation Process, *Chinese Journal of Rock Mechanics and Engineering*, *25* (2006), 3, pp. 467-472

[3] Wu, S., *et al.*, Analysis of Effective Stresses of Coal Containing Coal Bed Methane, *Chinese Journal of Rock Mechanics and Engineering*, *24* (2005), 10, pp. 1674-1678
[4] Brace, W. F., *et al.*, Dilatancy in the Fracture of Crystalline Rocks, *Journal of Geophysical Research*, *71* (1966), 16, pp. 3939-3953
[5] Li, P., *et al.*, A Volumetric Strain-Based Method to Determine Crack Initiation Stress of Low-Porosity Rocks, *Proceedings*, 5th International Conference on Intelligent Systems Design and Engineering Applications (ISDEA), Washington, DC, USA, 2014, pp. 106-108
[6] Peng, J., *et al.*, Crack Closure Stress and Damage Evaluation of Rock Microcrack, *Journal of Rock Mechanics and Engineering*, *34* (2015), 6, pp. 126-132
[7] Qiao, L., *et al.*, Study on the Lateral Strain Response for Determining Crack Initiation in Compression Tests on Low-Porosity Rocks, (Rock Characterization, Modelling and Engineering Design Methods), *Proceedings*, 3rd International Society for Rock Mechanics (ISRM) Sinorock Symposium, Shanghai, China, 2013, pp. 143-148
[8] Du, Y., *et al.*, Study on Triaxial Compression of Gas - Bearing Coal under Different Confining Pressure, *Coal Mine Safety, 45* (2014), 10, pp. 10-13
[9] Li, X., *et al.*, Experimental Study on Mechanical Properties of Ouburst Coal Containing Gas under Triaxial Compression (in Chinese), *Chinese Journal of Rock Mechanics and Engineering,* (2010), S1, pp. 3350-3358
[10] Ma, Z., *et al.*, Experimental Study on the Effect of Temperature on Coal Mechanical Properties, *Journal of Mining and Safety Engineering. 22* (2005), 3, pp. 46-48
[11] Shi, Y., *Applied Mathematical Statistics*, Xi'an Jiao Tong University Press, Xi'an, China, 2005
[12] Franklin, J. A., ISRM Suggested Methods for Determining the Strength of Rock Materials in Triaxial Compression: Revised Version, *International Journal of Rock Mechanics and Mining Sciences and Geo Mechanics Abstracts, 20* (1983), 6, pp. 285-290
[13] Eberhardt, E., *et al.*, Identifying Crack Initiation and Propagation Thresholds in Brittle Rock, *Canadian Geotechnical Journal*, *35* (1998), 2, pp. 222-233
[14] Martin, C. D., *et al.*, The Progressive Fracture of Lac Du Bonnet Granite, *International Journal of Rock Mechanics and Mining Sciences and Geo Mechanics Abstracts*, *31* (1994), 6, pp. 643-659
[15] Nicksiar, M., *et al.*, Evaluation of Methods for Determining Crack Initiation in Compression Tests on Low-Porosity Rocks, *Rock Mechanics and Rock Engineering, 45* (2012), 4, pp. 607-617

Paper submitted: February 10, 2017
Paper revised: May 10, 2017
Paper accepted: May 16, 2017